Chapter 17
Experimental Modal Analysis of an Additively Manufactured Model

Aditya Panigrahi, Brianna Blocher, Marc Eitner, and Jayant Sirohi

Abstract Additive manufacturing methods have advanced a lot in the past year. Methods like Fused Deposition Modeling (FDM) have gained popularity due to their versatility in material and minimal limitation on the geometry. Structural modeling of additively manufactured parts can, however, be complicated. This is primarily due to the dependence of material stiffness on print settings such as layer height, infill density, and infill pattern. In addition, the material can exhibit anisotropic characteristics due to parameters like the adhesiveness of layers, the orientation of the raft, and the layer deposition speed. This study conducts an experimental modal analysis on a 40% scaled model whose geometry is based on the aircraft Initial Concept 3.X (IC3X). The test article was manufactured using FDM, and ABS was chosen as the material. Fiber-optical strain sensors were attached to the test article and were used to record the response to structural excitation. Static tests were performed in addition to dynamic testing to further evaluate the test article's stiffness. The static test cases were used to update a finite element model of the test article and to obtain precise values of the Young's modulus, which is dependent on printer settings. The natural frequencies obtained from both the numerical model and dynamic testing showed good agreement.

Keywords FEA · Experimental modal analysis · Additive manufacturing · Fiber-optic · FDM

17.1 Introduction

Additive manufacturing (AM) is hailed as a significant revolution in manufacturing engineering due to its minimal geometry and materials limitations. Fused Deposition Modeling (FDM) has become an integral part of rapid prototyping among the various AM methods enabling engineers to produce complex parts. In FDM, a filament is pushed into a heated Liquidifier and is extruded through a nozzle. The nozzle is free to move along two orthogonal axes. The nozzle deposits the molten material onto a stage that can move up and down, which results in the material cooling down and solidifying. This process is carried out until all the layers are deposited on top of each other. For a hollow part, FDM considers the gap between the outer and inner geometry of the model and uses layers to fill that gap. The user can select parameters like the infill density, part orientation, and infill pattern based on the application. These parameters can heavily influence the mechanical properties of the printed part [1–3]. Raffic et al. [4] investigated the effect of these parameters on the tensile strength of ABS (acrylonitrile butadiene styrene). According to their research, infill density significantly increases the strength due to the increased strength provided by high infill density. Parts made with the FDM process exhibit anisotropic material behavior due to the orientation of the filament that is deposited at each layer of the part. Due to these parameters, a part fabricated using the FDM process can deviate substantially from the original design, typically more than a part made using conventional subtractive manufacturing processes (e.g., milling of metal).

It is essential that the effects of these printing parameters are evaluated. A common task for structural engineers is to match experimental data with a numerical model. This study investigates a large, 1.5 m-long 40% scale model of a hypersonic air vehicle manufactured using the FDM process. The model was instrumented with 23 fiber optical strain sensors, and static tests and modal analysis (impact testing) were performed. This study evaluates how well a large-scale FDM model matches static and dynamic numerical predictions (FEA).

A. Panigrahi (✉) · B. Blocher · M. Eitner · J. Sirohi
Department of Aerospace Engineering and Engineering Mechanics, The University of Texas at Austin, Austin, TX, USA
e-mail: aditya.panigrahi@austin.utexas.edu; brianna.blocher@austin.utexas.edu; marceitner@utexas.edu; sirohi@utexas.edu

M. Allen et al. (eds.), *Special Topics in Structural Dynamics & Experimental Techniques, Volume 5*,
Conference Proceedings of the Society for Experimental Mechanics Series, https://doi.org/10.1007/978-3-031-37007-6_17

17.2 Methodology

17.2.1 Initial Concept 3.X Vehicle (IC3X)

The Initial Concept 3.X Vehicle (IC3X) was designed by the Air Force Research Laboratories (AFRL) as part of an initial sizing study [5]. For this project, the IC3X was scaled down by 40% and used as a test article to conduct static and dynamic structural tests. The model was manufactured using a Stratasys Fortus 450MC^{TM}, which is a Fused Deposition Modeling machine capable of printing parts made out of materials like ABS (acrylonitrile butadiene styrene) and PLA (polylactic acid). ABS was chosen as the material for the IC3X test article.

The internal structure of the test article was explicitly designed to increase the sensitivity of internal strain sensors to bending moments. A thin wall section would lead to structural instability for a test article of this size, whereas a thick wall would increase the stiffness and provide a low signal-to-noise ratio. The solution to this problem was to implement localized reduction of wall thicknesses at intervals along the length of the model where the strain sensors were attached. This localized wall thickness reduction is referred to as a flexure region. Figure 17.1 shows the schematic of the test article, along with a magnified region that shows the flexure region. The test article was mounted on a metal sting, as shown in Fig. 17.2.

17.2.2 Experimental Setup

17.2.2.1 Fiber Optical Strain Sensors

As mentioned earlier, the flexure region is the ideal place to attach strain sensors. The system used for measuring the strain from the FBG fiber is called GTR FBG Interrogator (GTR1001-E) and have broad applications. For example, GTR 1001-E can be used on an airframe for shape sensing [6]. Each FBG measures strain at one location. Sensors embedded in the fiber operate at a 19.23 kHz sample rate and can record strain values as low as 1μ strain. Five channels or strings of FBG fibers are attached along the length of the IC3X model. Figure 17.3 shows a schematic of sensor locations.

17.2.2.2 Experimental Modal Setup

In this study, experimental modal analysis was conducted by using an impact hammer to excite the model, and the strain sensors were used to measure the response. The impact hammer (PCB 086B03) was connected to an NI DAQ system to record the impulse response. The red dot on Fig. 17.3 shows the impact location. Response from the impulse was recorded separately for each channel. A metal tip was attached to the hammer in order to improve the impact, and the response was measured at the sampling frequency of 19.23 kHz, same as the FBG system.

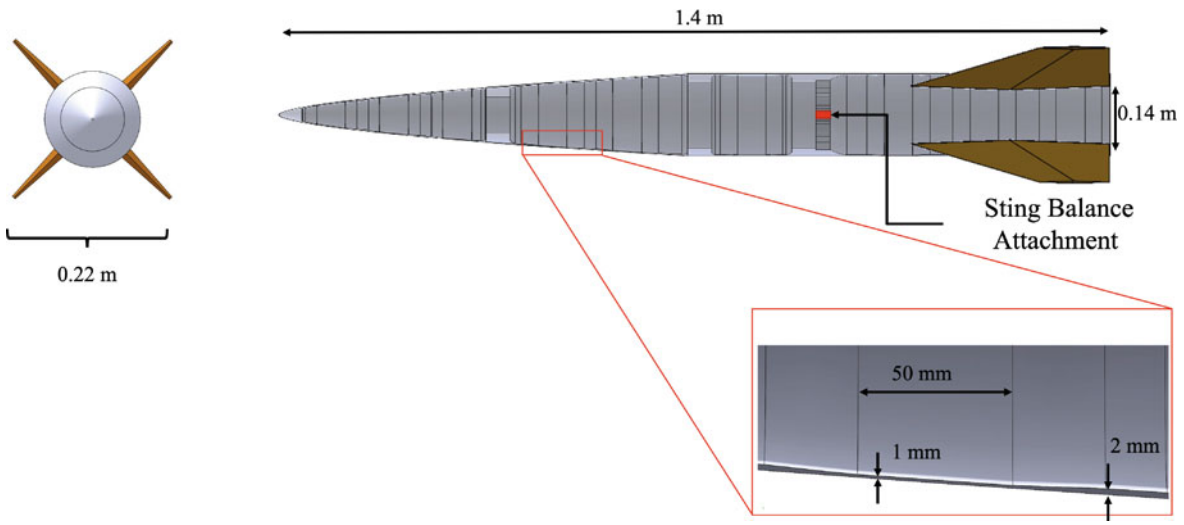

Fig. 17.1 IC3X 40% scale model test article

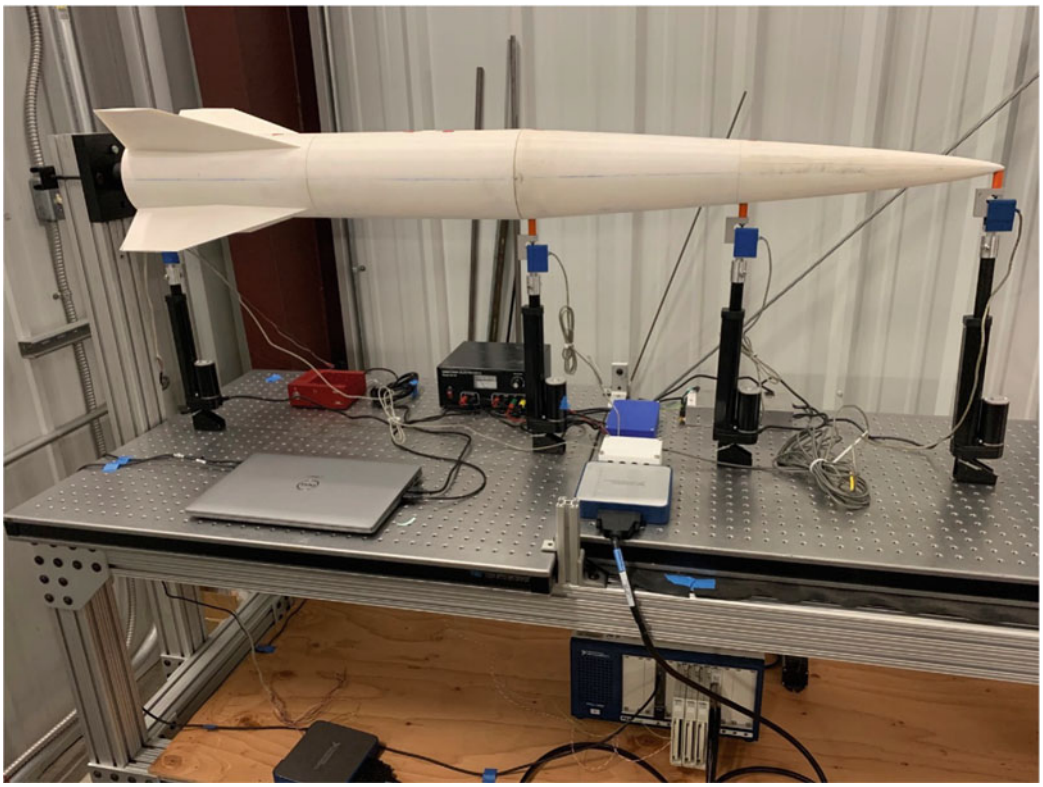

Fig. 17.2 Test article setup

17.2.3 Numerical Model

ANSYS mechanical module was used to develop a numerical model for the test article. A fixed boundary condition was applied to the faces interfacing with the sting. In ANSYS mechanical, the primary input is the static load applied on the test article, which ensures that the numerical model setup is as close as possible to the experimental setup.

17.3 Results and Discussion

17.3.1 Updating the Young's Modulus of ABS

The Young's modulus of an FDM material can vary based on the printer settings, as was discussed previously. While the ABS material used for the test article has a range for Young's modulus provided from its manufacturer (2.46 GPa-2.14 GPa), it was important for the numerical modeling to obtain a more accurate value.

For this study, a cylinder of length 0.34 m and a wall thickness of 2 mm was printed in the same printer with the same orientation and infill pattern as the IC3X test article. The cylinder was instrumented with conventional foil strain gages, and static loads were applied. Due to the simple geometry, it was possible to use the strain equation for a beam [7], as shown in Equation (17.1), from which Young's modulus was calculated. M is the bending moment, y is the radius between the neutral axis to the location of the strain gauge, I is the area moment of inertia, and $\epsilon_{measured}$ is the measured strain.

$$E_{Theo} = \frac{My}{\epsilon_{measured} I} \tag{17.1}$$

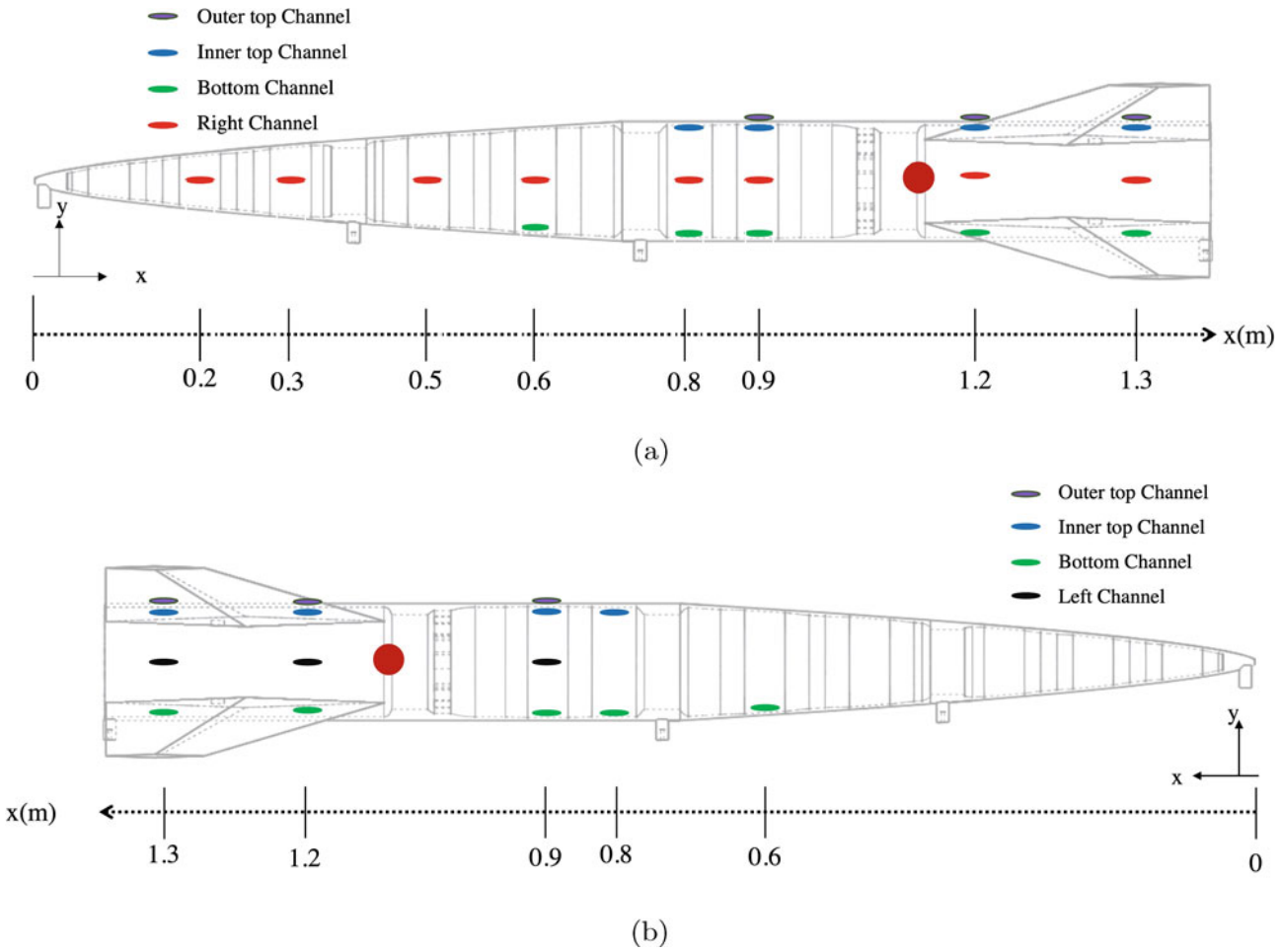

Fig. 17.3 Schematic of sensor placement on the IC3X. (**a**) Sensor placement (right side view). (**b**) Sensor placement (left side view)

A full bridge strain gage was applied 127 mm from the base. One end of the cylinder was clamped to enforce fixed boundary conditions, and weights were applied at the free end of the cylinder. The extracted Young's modulus from these strain measurements was 2.293 ± 0.0219 GPa, which was within the manufacturer-provided range. Thus, a Young's Modulus of 2.293 GPa was used in the FEA model.

17.3.1.1 Geometry Update

Due to the printer resolution, which results from the layer thickness of the FDM process, there are discrepancies in wall thickness between the CAD model and the final printed model. Since these discrepancies affect the area moment inertia, which affects the strain, the geometry used for the numerical solution must be updated to get a good agreement between the numerical model and experiments. In order to update the geometry, a linear actuator was used to apply a compressive force at the middle of the nose cone. Three strain sensors on the bottom channel were considered since they experienced bending moments. The thickness of the flexures was changed in the CAD software. Table 17.1 shows the changes in the wall thickness that were made to match the numerical solution to the experimental values. Figure 17.4 compares the strain calculated by the numerical model for the original and updated geometry for a single sensor. Small changes in wall thickness can have significant effects on the strain. This updated geometry and the new Young's Modulus were implemented on the numerical model.

Table 17.1 Geometry modifications after model updating

Location	Original (CAD) thickness [mm]	Updated (CAD) thickness [mm]
All thick parts	2.00	2.03
Most downstream flexure	1.5	1.51
All other flexures	1.0	0.91

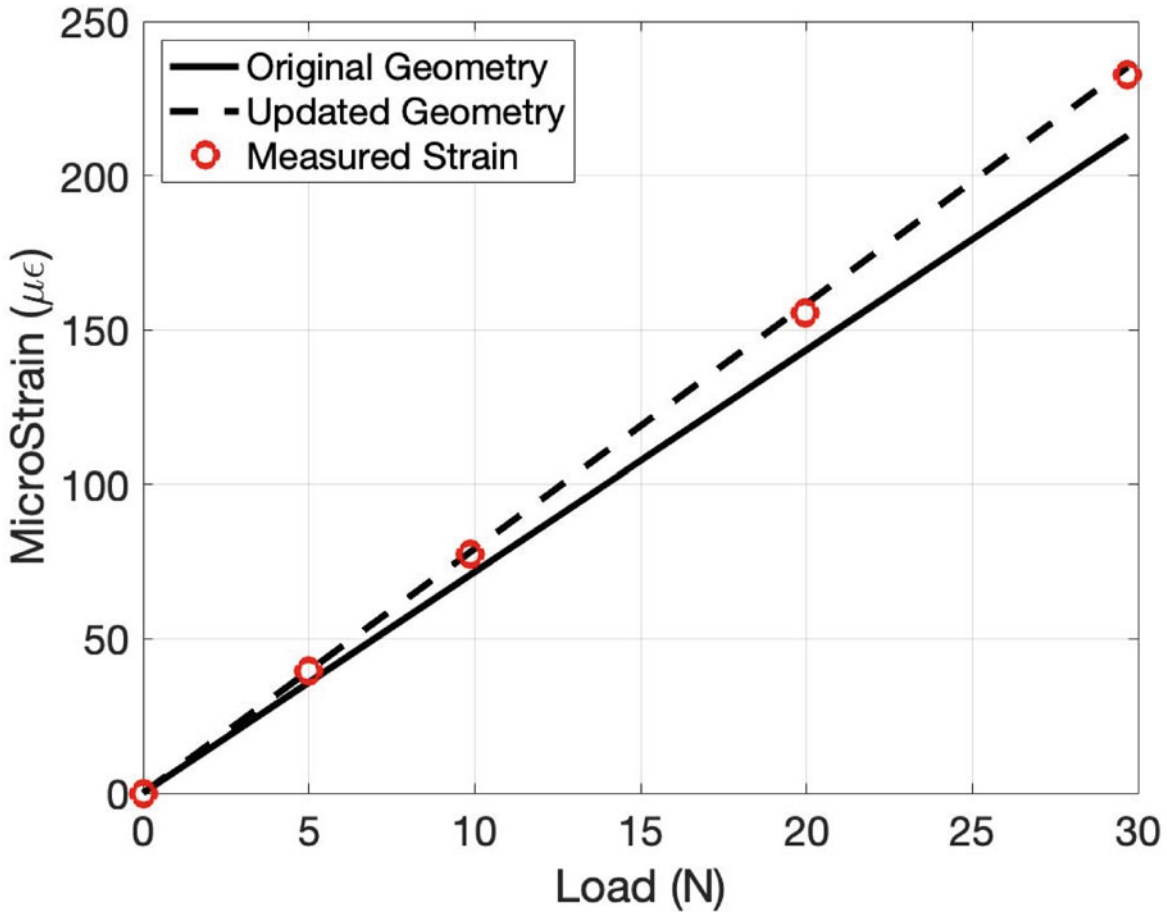

Fig. 17.4 Effect of changing flexure thickness on strain values from the numerical model

17.3.2 Frequency Response Functions

The modal parameters of the model were computed from the Frequency Response Functions (FRF), which were obtained from the measured strain and applied impulses. Figure 17.5 shows the power spectra of four impacts. They show minimal variation of magnitude for the considered frequency range of 0–300 Hz and were therefore selected to calculate the FRFs.

As mentioned earlier, four impacts were performed at the exact location for each channel shown in Fig. 17.3 and averaged to get an FRF for each sensor. Figure 17.6 shows the impulse and the resultant strain response for a single sensor. It can be seen that the impulse creates periodic strain response whose amplitude dies down as time goes on. This behavior was consistent in all of the sensors for all of the trials. A low-pass filter with a cut-off frequency of 700 Hz was applied to the signal to reduce the noise in the signal.

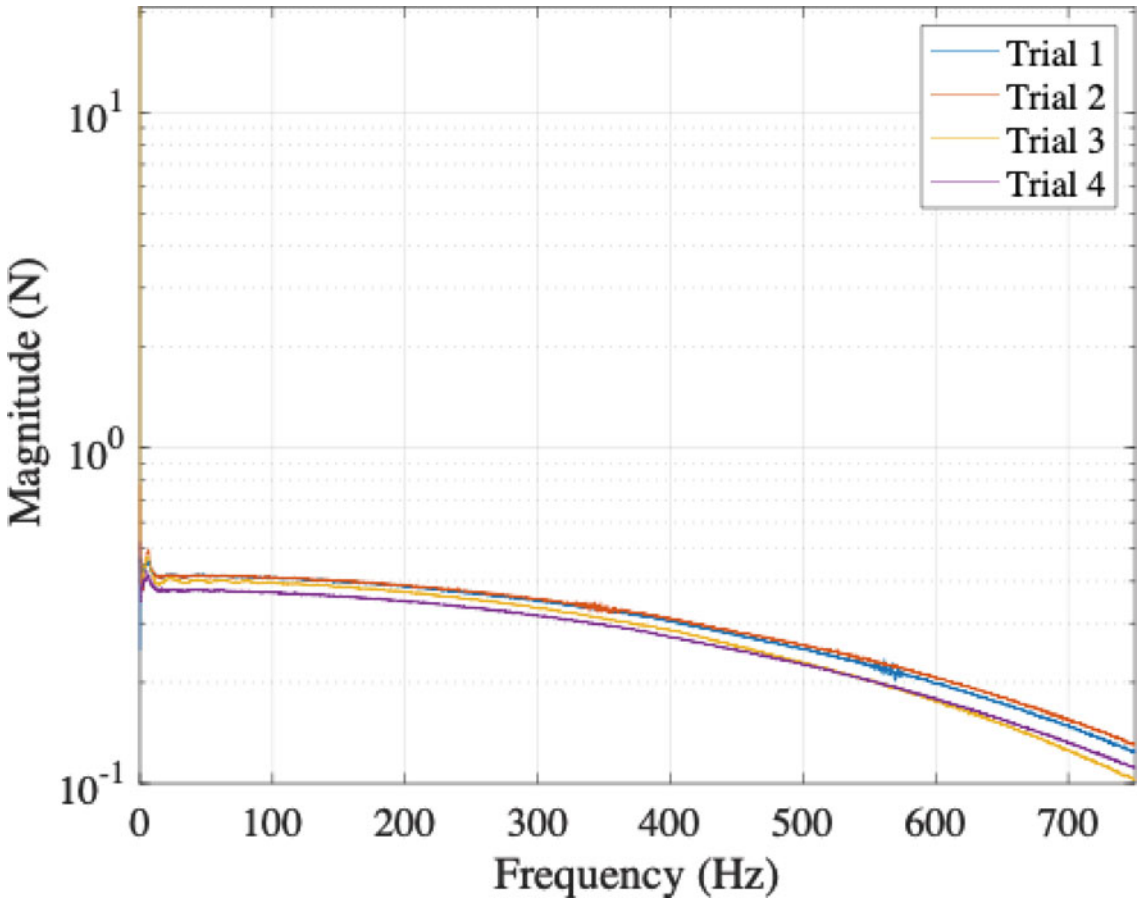

Fig. 17.5 Power spectra of impacts from impact hammer

Figure 17.7 shows the averaged FRF plotted over the FRFs of each trial for a single sensor. The averaged FRF appears clean and indicates a good signal-to-noise ratio of the measured data. The stabilization diagram for each FRF was computed using the MATLAB system identification toolbox. It was used to find the distinct stable peaks to identify the system's natural frequencies. Table 17.2 lists the natural frequencies determined from the stabilization diagrams of the FRFs of four sensors. These values are compared with the natural frequencies determined from the numerical FEA model.

17.4 Conclusion

Static tests resulted in geometry updates, significantly improving predictions model stiffness. Updating Young's Modulus and the flexure geometry helped generate more accurate strain values when compared to the static numerical model. For the dynamic testing part of this study, the modal analysis showed a good correlation in natural frequencies for both numerical and experiment values.

Structural dynamics of a large-scale part manufactured using additive manufacturing, like the test article of IC3X, is influenced by multiple parameters like infill density and pattern, which can affect the stiffness of the model, which in turn can affect the modes of the system. Therefore, a future study is planned in which the same rocket model is made from aluminum and will undergo the same model updating and modal analysis steps as in this study. A comparison of both results (ABS and aluminum model) will help identify issues related to the stiffness of large-scale FDM parts.

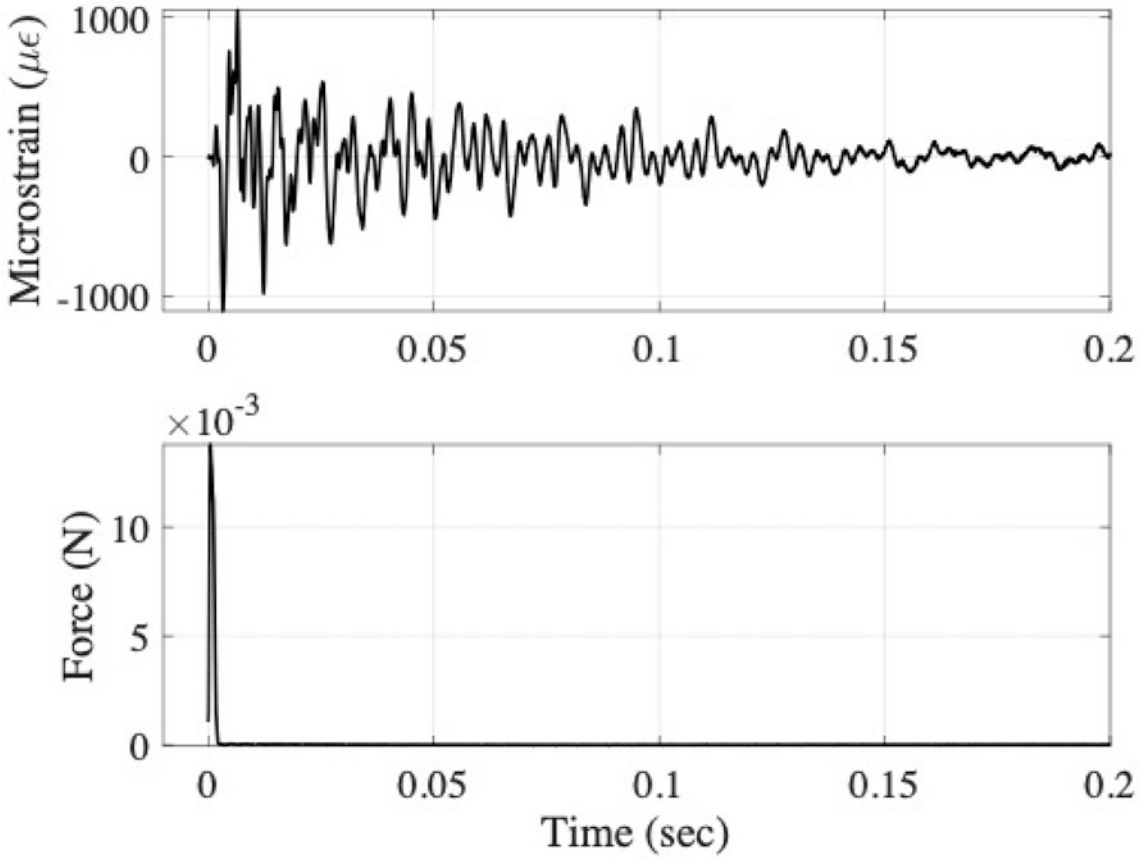

Fig. 17.6 Time histories of measured impact and strain, after low-pass filtering

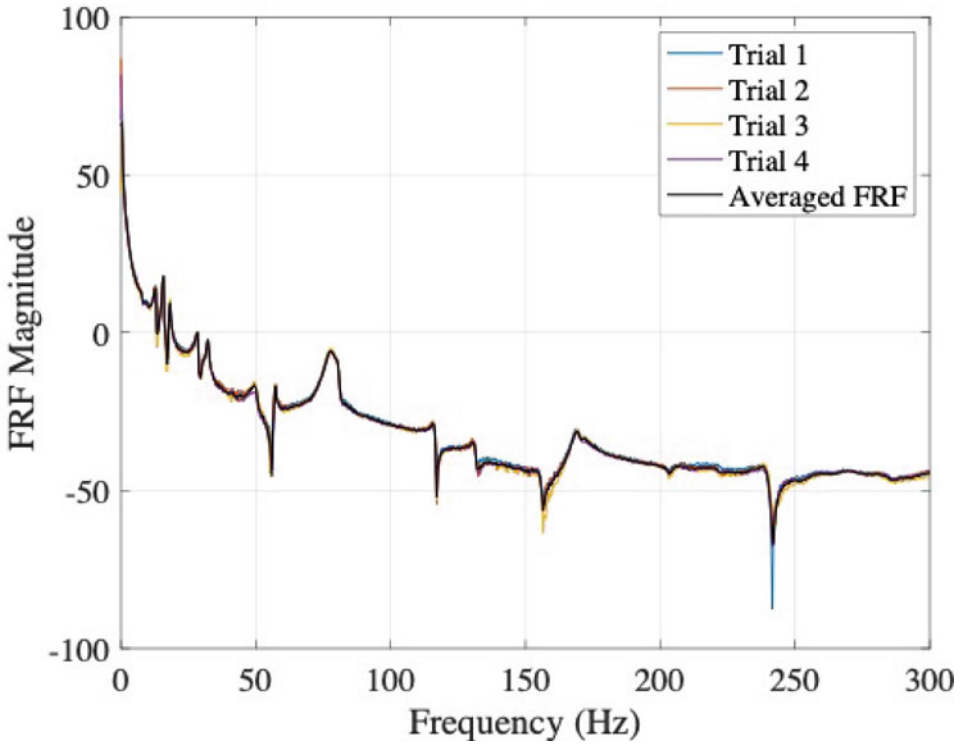

Fig. 17.7 Example of frequency response functions for multiple impacts

Table 17.2 Comparison of measured and calculated natural frequencies

Nat. frequency (FEA) [Hz]	Nat. Frequency (Experiment) [Hz]	% diff.
28.5	28.7	0.7
71.6	75.8	5.7
119.8	116.4	2.8
163.2	167.4	2.5

Acknowledgments This work was supported by AFOSR grant FA9550-21-1-0089 under the NASA University Leadership Initiative (ULI), with Dr. Sarah Popkin as program manager.

References

1. Bellini, A., Güçeri, S.: Mechanical characterization of parts fabricated using fused deposition modeling. Rapid Prototyping J. **9**, 252–264
2. Garg, A., Bhattacharya, A.: An insight to the failure of FDM parts under tensile loading: finite element analysis and experimental study. Int. J. Mech. Sci. **120**, 225–236 (2017)
3. Xue, F., Robin, G., Boudaoud, H., Cruz Sanchez, F.A., Daya, E.M.: Effect of process parameters on the vibration properties of PLA structure fabricated by additive manufacturing. In: 2021 International Solid Freeform Fabrication Symposium, University of Texas at Austin, 2021
4. Mohammed, R.N., Babu, K., Palaniappan, P.L., RajeshKannan, P., Venkatramanan, N.S.: Effect of FDM process parameters in ABS plastic material. Int. J. Mech. Prod. Eng. (2017) 895–903.
5. Klock, R.J.: Efficient numerical simulation of aerothermoelastic hypersonic vehicle. Ph.D. Thesis, University of Michigan (2017)
6. SensuronLLC.: Strain measurements comparison between distributed fiber optic sensing and strain gauges. https://www.sensuron.com/
7. Sadd, M.H.: Elasticity: Theory, Applications and Numerics, 4th edn. Elsevier, Amsterdam (2021)